Pathology (April 2019) **51(3)**, pp. 274–280

CHEMICAL PATHOLOGY

Role of protein structure in variant annotation: structural insight of mutations causing 6-pyruvoyl-tetrahydropterin synthase deficiency

Joao R. C. Muniz[1,*,†], Natalie Wing-sum Szeto[2,†], Rebecca Frise[1], Wen Hwa Lee[1], Xian-song Wang[2], Beat Thöny[3], Nastassja Himmelreich[4], Nenad Blau[4], Kwang-Jen Hsiao[5,6,7], Tze-Tze Liu[7,8], Opher Gileadi[1], Udo Oppermann[1,9], Frank Von Delft[1,10,11], Wyatt W. Yue[1,‡], Nelson Leung-sang Tang[2,‡]

[1]Structural Genomics Consortium, Nuffield Department of Medicine, University of Oxford, United Kingdom; [2]Department of Chemical Pathology and Li Ka Shing Institute of Health Sciences, The Chinese University of Hong Kong, Hong Kong; [3]Division of Metabolism, University Children's Hospital, Zurich, Switzerland; [4]Dietmar-Hopp Metabolic Center, University Children's Hospital, Heidelberg, Germany; [5]Department of Medical Research, Taipei Veterans General Hospital, Taiwan; [6]Preventive Medicine Foundation, Taipei, Taiwan; [7]Department of Education and Research, Taipei City Hospital, Taipei, Taiwan; [8]Genome Research Center, National Yang-Ming University, Taiwan; [9]Botnar Research Centre, Oxford Biomedical Research Unit, United Kingdom; [10]Diamond Light Source Ltd, Harwell Science and Innovation Campus, Didcot, United Kingdom; [11]Department of Biochemistry, University of Johannesburg, Auckland Park, South Africa; [*]current address: Sao Carlos Institute of Physics, University of Sao Paulo, Sao Carlos - SP, Brazil; [†]both authors contributed equally; [‡]both authors are corresponding authors

Summary

Genetic defects on 6-pyruvoyl-tetrahydropterin synthase (PTPS) are the most prevalent cause of hyperphenylalaninaemia not due to phenylalanine hydrolyase deficiency (phenylketonuria). PTPS catalyses the second step of tetrahydrobiopterin (BH_4) cofactor biosynthesis, and its deficiency represents the most common form of BH_4 deficiency. Untreated PTPS deficiency results in depletion of the neurotransmitters dopamine, catecholamine and serotonin causing neurological symptoms.

We archived reported missense variants of the *PTS* gene. Common *in silico* algorithms were used to predict the effects of such variants, and substantial proportions (up to 19%) of the variants were falsely classified as benign or uncertain. We have determined the crystal structure of the human PTPS hexamer, allowing another level of interpretation to understand the potential deleterious consequences of the variants from a structural perspective. The *in silico* and structure approaches appear to be complimentary and may provide new insights that are not available from each alone. Information from the protein structure suggested that the variants affecting amino acid residues required for interaction between monomeric subunits of the PTPS hexamer were those misclassified as benign by *in silico* algorithms. Our findings illustrate the important utility of 3D protein structure in interpretation of variants and also current limitations of *in silico* prediction algorithms. However, software to analyse mutation in the perspective of 3D protein structure is far less readily available than other *in silico* prediction tools.

Database reference: OMIM, 261640; PDB code, 3I2B.

Key words: 3D protein structure; mutation analysis; *in silico* prediction.

Abbreviations: BH_4, tetrahydrobiopterin; GTP, guanosine triphosphate; HPA, hyperphenylalaninaemia; PTPS, 6-pyruvoyl-tetrahydropterin synthase; *PTS*, 6-pyruvoyl-tetrahydropterin synthase gene; TCEP, Tris(2-Carboxyethyl) phosphine hydrochloride.

Received 14 September, revised 13 November, accepted 19 November 2018
Available online 8 March 2019

INTRODUCTION

Defects in the phenylalanine metabolism are important inherited metabolic diseases (IMD) causing neurological deficits and intellectual disability. Deficiency in phenylalanine hydroxylase causing classical phenylketonuria (PKU) is the most prevalent worldwide (about 1:10,000 live births).[1] Disorders leading to tetrahydrobiopterin (BH_4) deficiency are the next most common aetiology of hyperphenylalaninaemia (HPA). BH_4 is an essential cofactor for nitric oxide synthase, alkylglycerol monooxygenase, and four aromatic amino acid monooxygenases, the latter being essential for the hepatic degradation of phenylalanine and synthesis of neurotransmitter precursors of catecholamine and serotonin.[2,3] BH_4 deficiency represents a heterogenous group of rare neurological diseases due to defective biosynthesis and recycling of BH_4, where patients present with deficiency of brain catecholamine and, with the exception of sepiapterin reductase deficiency and autosomal dominant

Print ISSN 0031-3025/Online ISSN 1465-3931
DOI: https://doi.org/10.1016/j.pathol.2018.11.011

guanosine triphosphate cyclohydrolase deficiency (Segawa disease), with HPA.[4,5] Clinical and biochemical data of more than 1,100 patients with inherited BH_4 deficiencies are tabulated in the BIODEF database (http://www.biopku.org).[6] This condition is also particularly prevalent in some ethnic groups in Southeast Asian populations in Southern China, Taiwan, and Thailand.[7]

Autosomal recessive variants on *PTS* (Entrez Gene 5805) that lead to 6-pyruvoyl-tetrahydropterin synthase (PTPS) deficiency (OMIM 261640) account for the majority of BH_4 defects worldwide (prevalence is about 1:500,000 live births).[8] The human *PTS* gene maps to chromosome location 11q22.3–q23.3, and consists of six exons encoding a 145 amino acid protein.[9] The PTPS enzyme (EC 4.6.1.10) catalyses the second reaction of the three-step *de novo* synthesis of BH_4 from guanosine-5′-triphosphate (GTP), namely the conversion of 7,8-dihydroneopterin triphosphate to 6-pyruvoyl-tetrahydropterin.[3] The severe form of PTPS deficiency causes HPA and developmental delay associated with low birthweight and parkinsonian-like features,[6,10] while the less common mild form gives rise to HPA only with no neurological involvement.[11] PTPS-deficient patients require a combined treatment with BH_4 to control the HPA, as well as neurotransmitter precursors (such as L-dopa/Carbidopa and 5-hydroxytryptophan) to replenish their deficit in the central nervous system,[12] although the outcome can be variable.[13]

Over 100 variants associated with PTPS deficiency have been reported,[5] most of which are missense variants, while others include termination and splicing variants. While the consequence of nonsense and frame-shift variants are easy to predict, they account for less than 10% of variants. ClinVar (https://www.ncbi.nlm.nih.gov/clinvar/?term=PTS%5Bgene%5D) is also an important database for disease-causing mutations. Missense variants lead to substitution of single amino acids at a particular codon, and their consequences can range from absolutely benign (such as those SNPs prevalent in the population) to deleterious and disease-causing. With the transformation of next-generation sequencing from a research tool to a clinical service, there is an explosion of sequence variant data in need of high throughput prediction of pathogenicity. In the past, sequence variants can be curated manually, and their inheritance can be traced in the pedigree. With hundreds of missense variants produced from a typical exome sequence data, we have to rely on pathogenicity prediction programs such as SIFT, PolyPhen and CADD score.[14–16] Therefore, the performance or accuracy of these commonly-used algorithms is the key to making the correct curation. Previous studies showed various limitations of these programs which had both false positive and false negative predictions.[17,18] A high proportion of missense mutations were classified as variants of uncertain significance.[19]

To this end, we present the crystal structure of the human homo-hexameric enzyme PTPS for the first time here, providing an unprecedented opportunity to assess the performance of commonly used variant prediction programs on an archive of patients' variants of PTPS. Although the murine PTSP structure had been solved previously and is known to be a homo-hexameric Zn(II)-metallo-enzyme, the structure of the human homologue had not been available until now.[20] With a focus on missense variants, this study aims to determine if information from an experimentally-determined protein structure could be helpful in understanding the mechanisms of deleterious variants.

MATERIALS AND METHODS

Archive of reported missense variants in patients of PTPS deficiency

Missense variants were retrieved from multiple sources, including UniProt (http://www.uniprot.org/uniprot/Q03393), BioMDB (http://www.biopku.org/home/docs/PTS.pdf), and ClinVar (https://www.ncbi.nlm.nih.gov/clinvar/?term=PTS%5Bgene%5D). A PubMed search was carried out to identify the original publications reporting these variants, and the patients' phenotypes were also recorded.

Only missense variants were included for further analysis and comparison of the performance of conservation-based prediction algorithms and HOPE curation using 3D protein structure.[21]

Structure determination of human PTPS

Expression, purification and crystallisation

A DNA fragment encoding residues 8–145 of human PTPS (GenBank 4506331) was subcloned into pNIC28-Bsa4 vector (GenBank EF198106) incorporating an N-terminal His_6-tag. The plasmid was transformed into BL21(DE3)-R3-pRARE2, cultured in Terrific Broth at 37°C, and induced with 0.1 mM IPTG for overnight growth at 18°C. Cells were homogenised, centrifuged to remove cell debris, and purified by immobilised metal affinity (IMAC) and size-exclusion chromatography. Prior to crystallisation, the His-tag was removed by His-tagged TEV protease and subsequently purified by IMAC. Protein was concentrated to 17.75 mg/mL and stored in 20 mM HEPES pH 7.5, 150 mM NaCl, 5% glycerol. Crystals were grown by vapour diffusion at 4°C in sitting drops mixing 75 nL protein and 75 nL reservoir solution containing 20% PEG 3350 and 0.2 M magnesium formate. Crystals were cryo-protected in mother liquor containing 25% (w/v) ethylene glycol and flash-cooled in liquid nitrogen.

Data collection and structure determination

Diffraction data to 2.30 Å resolution were collected on beamline X10SA at the Swiss Light Source, and processed using the CCP4 Program suite.[22] The structure of hPTPS was solved by molecular replacement with PHASER,[23] using the rat liver PTPS structure as search model (PDB code 1GTQ, ~80% sequence identity).[24] Initial automated model building was performed with ARP/wARP,[25] followed by cycles of iterative manual model building with COOT[26] and REFMAC5 refinement.[27] The active site metal ion was modelled as Ni(II), based on known leaching effect from nickel affinity resin in the IMAC step. The final structure factors and coordinates were deposited in the Protein Data Bank under the accession code 3I2B (Supplementary Table 1, Appendix A). Figures 1 and 2 showing the 3D structure models were generated using the program ICM (www.molsoft.com).

Testing the accuracy of *in silico* prediction of archived missense variants

SIFT (Sorting Intolerant from Tolerant[28]) and PolyPhen-2[14] are two commonly used online tools that are used to predict whether non-synonymous single amino acid polymorphisms may be deleterious and may affect protein function. SIFT is mainly a sequence homology based method which estimates evolutionary conservation of residues,[29] and it works by blasting the query sequence against the non-redundant protein database at NCBI or UniProt[30] for functionally related homologous proteins. Upon sequence alignment, the program calculates the probabilities of observing the individual 20 possible amino acids in each position in the alignment, normalises these probabilities by the most frequently naturally occurring amino acid at that position, and derives a scoring matrix from the data across species. An amino acid substitution will be classified as deleterious if the SIFT score, which is the scaled-probability of observing the particular amino acid substitution among homologous proteins, lies below a cut-off threshold, for example 0.05. The closer the score is to 0, the higher the probability the variant may be deleterious. SIFT achieved a 69% true positive rate when tested in the human diseased dataset,[31] while it had a 19% false positive rate[28] in the healthy human test dataset.[32]

On the other hand, PolyPhen-2 integrates results from 11 prediction algorithms, eight of which are sequence-based and three of which are structure-

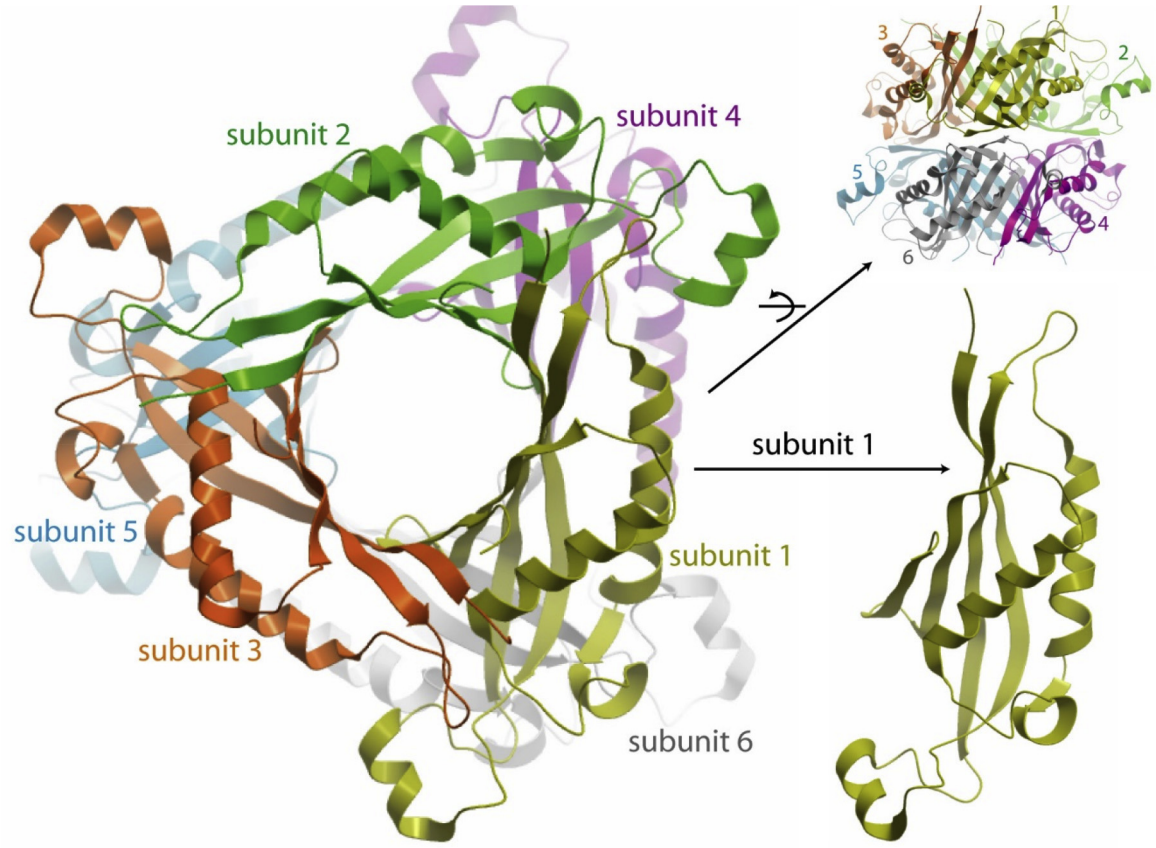

Fig. 1 Ribbon diagram of human 6-pyruvoyl-tetrahydropterin synthase (PTPS) structure illustrating the homo-hexameric assembly. The six subunits are coloured distinctively.

based, and reports a naïve Bayes probability that the substitution is damaging. This was carried out in an attempt to classify the concerned substitution into one of the three classes: benign (probability 0.0–0.15), possibly damaging (0.15–1.0), or probably damaging (0.85–1.0). The closer the probability is to 1, the more likely that the variant may be damaging. PolyPhen-2 had been trained by two datasets present in UniProt, namely HumVar and HumDiv. The former is compiled from human disease-causing alleles paired with related non-damaging alleles within closely related mammalian homologues, while the latter consists of human disease alleles paired with human alleles that are not involved in disease. HumVar-trained and HumDiv-trained PolyPhen-2 achieved 73% and 92% true positive rates in an assessment of their accuracies, but with a false positive rate of 20%. The former is recommended for diagnosing Mendelian diseases with highly deleterious variants, while the latter is more sensitive and will classify even mildly deleterious variants as damaging.[14]

Using HOPE program to curate variants against 3D protein structure

HOPE is a web-based platform[21] that allows users to enter missense variants and it helps to map them to the 3D protein structure and provides curation on the potential effects on the known or predicted functional domains.[33–35] Previous evaluation by the program developing team showed promising results with the dbSNP datasets. Here we tried to see if it provided new insights to those variants that were missed by SIFT and PolyPhen-2 (false negative variants, Fig. 3). Default parameters in the HOPE program were used in our analysis.

RESULTS AND DISCUSSION

3D protein structure of PTPS

As part of a structural genomic effort to understand variants in human proteins involved in inborn errors of metabolism, the structure of hPTPS is determined at 2.3 Å resolution by X-ray crystallography. The hPTPS protomer (amino acids 8–144) has an elongated shape formed by a four-stranded β-sheet flanked by helices, bearing overall similarity with the previously reported murine structure.[24,36] hPTPS forms a hexameric structure comprising a dimer of trimers arranged in a head-to-head manner (Fig. 1), resulting in a central 12-stranded β-barrel pore as seen in PTPS homologues.[20,24,36] Each of the six active sites in the hPTPS hexamer is located at the interface of three subunits, where it harbours (1) three conserved histidines (His24, His49 and His51) to coordinate the divalent metal ion, previously characterised as Zn(II) in the murine structure;[24,36] (2) an inter-subunit triad of Cys43-Asp89-His90 that have been attributed as proton donors and acceptors during catalysis; and (3) a Ser/Thr-Glu motif (Thr107-Glu108 in hPTPS) involved in substrate binding.[20]

Archive of missense variants of *PTS*

To date, there are over 90 missense alleles reported to cause the severe or mild types of PTPS deficiency (Supplementary Table 2, Appendix A; and references therein), in addition to several splice site variants.[37,38] A majority of the missense variants are situated at evolutionarily conserved amino acid positions, indicating that they likely affect the function and activity of the enzyme. Among these, Asn36 and His49 are strictly invariant residues; His49 is one of the three metal coordinating histidines, while Asn36 interacts with nearby residues to maintain the structural integrity of an α-helix that lines the active site pocket. Variants of either residue (Supplementary Table 2, Appendix A; N36K, H46R, and His49Q) resulted in the severe form of PTPS deficiency.[39–41]

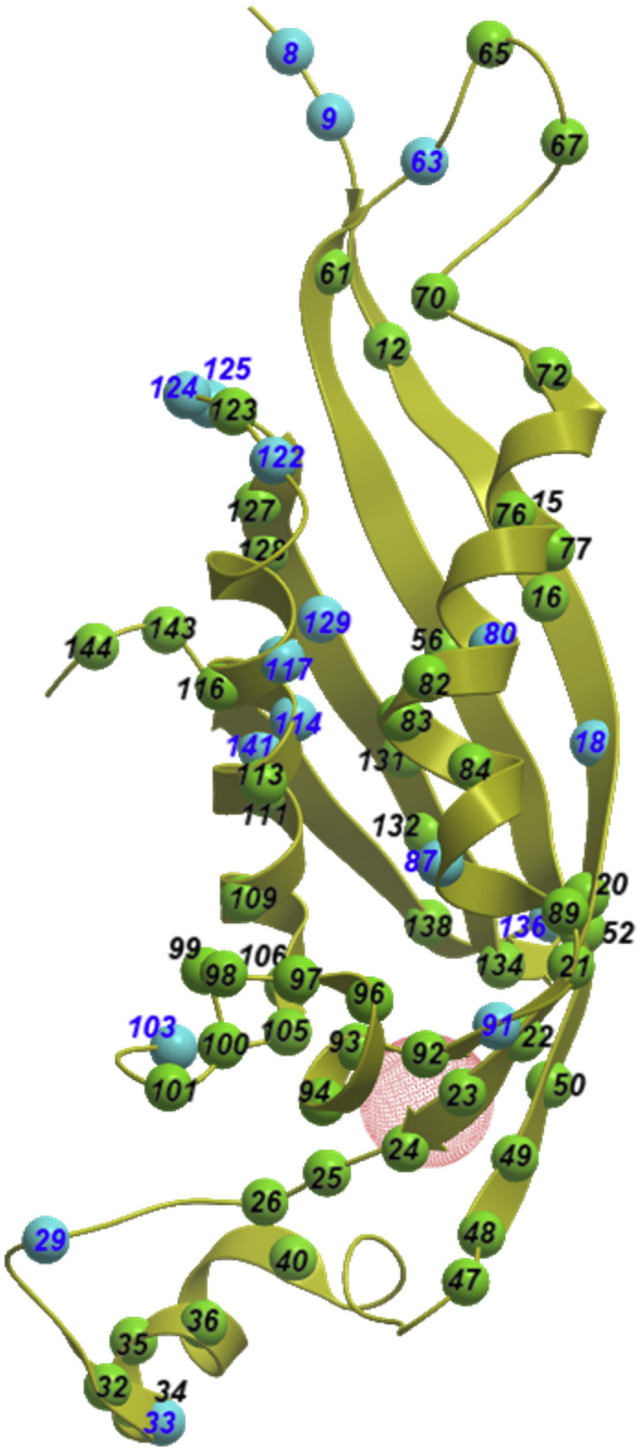

Fig. 2 Clustering of human 6-pyruvoyl-tetrahydropterin synthase (PTPS) missense variants. The positions of amino acid variants in one PTPS protomer are indicated by spheres and numbered according to their residue number. Mutation sites described in Fig. 3 are shown in cyan spheres; the remainder are shown in green spheres. The active site divalent metal ion is shown in the red sphere.

Performance of *in silico* variant effect prediction

SIFT and PolyPhen-2 are among the variant prediction methods that are of highest speed and ease of use.[42] However, SIFT is incapable of processing very long sequences.[43] On the other hand, although the sensitivity (true positive rate) of both SIFT and PolyPhen-2 were reported to have high sensitivity, the specificity (true negative rate) might be only around 0.5.[44]

As we are interested in the application of protein structure in this process, we confined to only missense variants found in PTPS patients. In keeping with previous evaluations, neither program had a perfect sensitivity to identifying deleterious variants. Among 95 variants in Supplementary Table 2 (Appendix A), SIFT and PolyPhen-2 identified 59% (56/95) and 52% (67/95) (using 'possibly damaging' as cut-off) as deleterious, respectively. With the latest reporting guideline requiring concordance of prediction programs output before variants are called deleterious, the sensitivity requiring concordance between both programs reduced to 51% (48/95). Such level of sensitivity was similar to that previously reported using whole genomes single nucleotide polymorphisms or Human Genetic Mutations datasets. Those variants which were wrongly predicted as benign did not cluster together or show any recognisable features as a group.

Overview of variants mapped to the 3D protein structure

Mapping of the known missense variants onto the human PTPS structure shows that they are broadly distributed along the entire length of the polypeptide (Fig. 2). It becomes apparent that many are clustered in the BH_4 binding region of the active site, representing a region of 'variantal hotspot'. These variants are likely to disrupt (1) the binding interactions with the BH_4 substrate (e.g., H49R, H49Q), or (2) integrity of secondary structure elements that contribute important residues to the active site (e.g., P87S, K91E). Away from the hotspot region, further variants can be found in the central β-barrel pore (e.g., I18T). With the active site and the supporting structure defined, many variants could be accounted by disruption of such important structure.

In order to see if an automatic variant interpretation algorithm based on 3D protein structure provides additional information, 20 disease-causing variants misdiagnosed (false negative) by both SIFT and PolyPhen-2 (Supplementary Table 2, Appendix A) were subjected to the HOPE algorithm, a web-based platform for structure-guided variant analysis. It turns out that HOPE has given more detailed analyses of the 20 variants that were missed by both SIFT and PolyPhen-2. A summary of the additional information derived from HOPE is given in Fig. 3. As HOPE does not generate a simple score to predict if a variant is being deleterious by using the 3D structure alone, we used it to gain insight into why these 20 of 95 (21%) variants were falsely classified as benign by either SIFT or PolyPhen-2. Figure 3 lists those variants that were false negative results of these two algorithms. It was found that disruption of either protein-protein contact or protein-ligand contact represented a large proportion of them. Twenty percent of the codon position with false negative predictions were in the vicinity of metal contact, and 20% of the substituted amino acids were not of the right side-chain length to make multimer contacts. The consequence of changes in side-chain lengths, resulting in loss of ability of the mutated residues to make contacts, could only be observed by prediction software which utilised 3D protein structure analysis such as HOPE, but not SIFT and PolyPhen-2. Similarly, the prediction by HOPE showed that half of the false predictions affected the protein's secondary structure or intramolecular bonding. Thirty percent involved

	Features of PTPS (such as 3D structure and monomer interactions) that are potentially affected by the variants, as suggested by HOPE analysis				**Grouping/classification of the variant based on HOPE analysis**	
	Involved in multimer contact	In the vicinity of metal contact	Forms structure	Forms salt bridge	Location of variant in protein	Variant observed in homologous proteins
R8L	Mutated residue becomes too small to form multimer contact; Change in hydrophobicity affects hydrogen bonding at multimeric contacts			Mutated residue changes from positively charged to neutral, disrupting ionic interaction at salt bridge	Surface	No
R9H	Mutated residue becomes too small to form multimer contact			Mutated residue changes from positively charged to neutral, disrupting ionic interaction at salt bridge	Surface	Yes
I18T					Core	Yes
K29T			Wild-type residue prefers alpha-helix but mutated residue doesn't		NA	Yes
D33G			Mutated residue (Asp) loses the flexibility that the wild-type residue (Gly) possesses for specific protein function	Mutated residue changes from negatively charged to neutral, disrupting ionic interaction at salt bridge	Surface	No, but residues with similar properties have been observed so variant may be false accepted as benign
I63V	Mutated residue becomes too small to form multimer contact				Surface	Yes
M80V			Wild-type residue prefers alpha-helix but mutated residue doesn't		Core	Yes
M80I			Wild-type residue prefers alpha-helix but mutated residue doesn't		Core, creates empty space	Yes
P87L			Mutated residue (Leu) loses the rigidity that the wild-type residue (Pro) possesses for special backbone conformation		Surface	Yes
K91R		Neighbouring residue makes metal contact and may be affected by the variant		Mutated residue has no change in property but wild-type residue is involved in salt bridge formation	Close to active site	Yes
V103A			Wild-type residue prefers beta-strand but mutated residue doesn't, destabilising local conformation		Surface	Yes
I114V		Neighbouring residue makes metal contact and may be affected by the variant			Core	Yes

Fig. 3 List of clinically reported variants that were false negative results on SIFT and PolyPhen-2 (misclassified as benign). 3D protein structure provides additional information about their potential effects, as shown in cyan spheres in Fig. 2.

N117L		Neighbouring residue makes metal contact and may be affected by the variant	Loss of hydrogen bonding after variant in the core of the protein disturbs correct folding		Core	Yes
L122I					Core	Yes
V124L					Surface	Yes
G125R			Mutated residue (Arg) loses the flexibility that the wild-type residue (Gly) possesses for specific protein function	Mutated residue changes from neutral to positively charged, disrupting ionic interaction at salt bridge	Surface	No
G125E			Mutated residue (Glu) loses the flexibility that the wild-type residue (Gly) possesses for specific protein function	Mutated residue changes from neutral to negatively charged, disrupting ionic interaction at salt bridge	Surface	Yes
K129E					Surface	Yes
D136G	Mutated residue becomes too small to form multimer contact		Mutated residue (Gly) loses the rigidity that may be required by the protein at this position	Mutated residue changes from negatively charged to neutral, disrupting ionic interaction at salt bridge	Surface	Yes
V141F		Neighbouring residue makes metal contact and may be affected by the variant			Surface	Yes

Fig. 3 (*continued*)

charge differences which potentially disrupted salt bridge (hydrogen bond) formation. In addition, K91R[7] was found to be located close to the active site, thus could be damaging to the protein's function. Eighty-five percent were among the observed residue types at the respective positions in homologous sequences, which could have been the cause of false negative results by conservation algorithms, as residue occurrence among homologous proteins is an important criterion for other prediction software like SIFT.[28]

New analysis methods are needed to interpret variant effect on protein structure

Today, when structures of most proteins are available one way or another, we propose to make use of this resource to curate single nucleotide variants and visualise the effects of amino acid substitutions at any codon position. In the past, when the list of variants had few entities, it was performed by manual inspection of the protein structure using PDB viewer tools. One could accommodate the side chain of the new amino acid in the existing protein and calculate a predicted steric hindrance. However, these predictions were not standardised, thus it was difficult to predict if such substitution could be accommodated.[45] Structure-guided pathogenicity prediction is not an easy task, also because the understanding of how protein structures bring to functions is still at its infancy.

Nowadays, as a typical WES generates a list of hundreds of missense variants, manual inspection of the protein structure is no longer feasible and some automatic curation of the protein structure is needed. Using structure-guided prediction involving web-based tools such as HOPE is a good start, but its prediction function is still limited and needs information feed from homology. Other groups have tried to make use of neural network and other algorithms to solve the classification problem.[33,46,47] However, their results still need validation in larger scale and feedback from more users. User-friendly 3D structure mutation analysis tools are still lacking, but it is believed that they deserve attention for future variant studies.

Acknowledgements: Help in X-ray data collection by staff at the Swiss Light Source is gratefully acknowledged. We thank David Meili and Corinne Gemperle for technical assistance on patients' variant analyses.

Conflicts of interest and sources of funding: The Structural Genomics Consortium is a registered charity (Number 1097737) funded by the Canadian Institutes for Health Research, the Canada Foundation for Innovation, Genome Canada through the Ontario Genomic institute, GlaxoSmithKline, Karolinska Institutet, the Knut and Alice Wallenberg Innovation, Merck and Co., Inc., the Novartis Research Foundation, the Swedish Agency for Innovation Systems, the Swedish Foundation for Strategic Research and the Wellcome Trust. This work is also supported in part by the Swiss National Science Foundation grant no. 31003A-119982 (to BT). This work is part of the RD-CONNECT initiative and was supported by the FP7-HEALTH-2012-INNOVATION-1 EU Grant No. 305444 and funding from the Dietmar Hopp Foundation (both to NB). The authors state that there are no conflicts of interest to disclose.

APPENDIX A. SUPPLEMENTARY DATA

Supplementary data to this article can be found online at https://doi.org/10.1016/j.pathol.2018.11.011.

Address for correspondence: Nelson L. S. Tang and Wyatt W. Yue, Department of Chemical Pathology, Room 38061, 1/F, Lui Che Woo Clinical Sciences Building, Prince of Wales Hospital, Shatin, New Territories, Hong Kong. E-mails: nelsontang@cuhk.edu.hk, wyatt.yue@sgc.ox.ac.uk

References

1. Blau N, VanSpronsen FJ, Levy HL. Phenylketonuria. *Lancet* 2010; 376: 1417–27.
2. Blau N, Thöny B, Cotton RGH, *et al*. Disorders of tetrahydrobiopterin and related biogenic amines. In: Scriver CR, Beaudet AL, Sly WS, *et al*., editors. *The Metabolic and Molecular Bases of Inherited Disease*. 8th ed. New York: McGraw-Hill, 2001; 1725–76.
3. Werner ER, Blau N, Thöny B. Tetrahydrobiopterin: biochemistry and pathophysiology. *Biochem J* 2011; 438: 397–414.
4. Longo N. Disorders of biopterin metabolism. *J Inherit Metab Dis* 2009; 32: 333–42.
5. Thöny B, Blau N. Mutations in the BH4-metabolizing genes GTP cyclohydrolase I, 6-pyruvoyl-tetrahydropterin synthase, sepiapterin reductase, carbinolamine-4a-dehydratase, and dihydropteridine reductase. *Hum Mutat* 2006; 27: 870–8.
6. Opladen T, Hoffmann GF, Blau N. An international survey of patients with tetrahydrobiopterin deficiencies presenting with hyperphenylalaninaemia. *J Inherit Metab Dis* 2012; 35: 963–73.
7. Chiu YH, Chang YC, Chang YH, *et al*. Mutation spectrum of and founder effects affecting the PTS gene in East Asian populations. *J Hum Genet* 2012; 57: 145–52.
8. Blau N. Genetics of Phenylketonuria: then and now. *Hum Mutat* 2016; 37: 508–15.
9. Kluge C, Brecevic L, Heizmann CW, *et al*. Chromosomal localization, genomic structure and characterization of the human gene and a retropseudogene for 6-pyruvoyltetrahydropterin synthase. *Eur J Biochem* 1996; 240: 477–84.
10. Jäggi L, Zurflüh MR, Schuler A, *et al*. Outcome and long-term follow-up of 36 patients with tetrahydrobiopterin deficiency. *Mol Genet Metab* 2008; 93: 295–305.
11. Niederwieser A, Shintaku H, Leimbacher W, *et al*. 'Peripheral' tetrahydrobiopterin deficiency with hyperphenylalaninaemia due to incomplete 6-pyruvoyl tetrahydropterin synthase deficiency or heterozygosity. *Eur J Pediatr* 1987; 146: 228–32.
12. Ogawa A, Kanazawa M, Takayanagi M, *et al*. A case of 6-pyruvoyl-tetrahydropterin synthase deficiency demonstrates a more significant correlation of L-Dopa dosage with serum prolactin levels than CSF homovanillic acid levels. *Brain Dev* 2008; 30: 82–5.
13. Chien Y, Chiang S, Huang A, *et al*. Treatment and outcome of Taiwanese patients with 6-pyruvoyltetrahydropterin synthase gene mutations. *J Inherit Metab Dis* 2001; 24: 815–23.
14. Adzhubei IA, Schmidt S, Peshkin L, *et al*. A method and server for predicting damaging missense mutations. *Nat Methods* 2010; 7: 248–9.
15. Kircher M, Witten DM, Jain P, *et al*. A general framework for estimating the relative pathogenicity of human genetic variants. *Nat Genet* 2014; 46: 310–5.
16. Vaser R, Adusumalli S, Leng SN, *et al*. SIFT missense predictions for genomes. *Nat Protoc* 2016; 11: 1–9.
17. Gnad F, Baucom A, Mukhyala K, *et al*. Assessment of computational methods for predicting the effects of missense mutations in human cancers. *BMC Genom* 2013; 14 (Suppl 3): S7.
18. Ghosh R, Oak N, Plon SE. Evaluation of in silico algorithms for use with ACMG/AMP clinical variant interpretation guidelines. *Genome Biol* 2017; 18: 225.
19. Moghadasi S, Eccles DM, Devilee P, *et al*. Classification and clinical management of variants of uncertain significance in high penetrance cancer predisposition genes. *Hum Mutat* 2016; 37: 331–6.
20. Ploom T, Thöny B, Yim J, *et al*. Crystallographic and kinetic investigations on the mechanism of 6-pyruvoyl tetrahydropterin synthase. *J Mol Biol* 1999; 286: 851–60.
21. Venselaar H, teBeek TA, Kuipers RK, *et al*. Protein structure analysis of mutations causing inheritable diseases. An e-Science approach with life scientist friendly interfaces. *BMC Bioinformat* 2010; 11: 548.
22. CCP4. CCP4 suite: programs for protein crystallography. *Acta Crystallogr D Biol Crystallogr* 1994; 50: 760–3.
23. McCoy AJ, Grosse-Kunstleve RW, Storoni LC, *et al*. Likelihood-enhanced fast translation functions. *Acta Crystallogr D Biol Crystallogr* 2005; 61: 458–64.
24. Nar H, Huber R, Heizmann CW, *et al*. Three-dimensional structure of 6-pyruvoyl tetrahydropterin synthase, an enzyme involved in tetrahydrobiopterin biosynthesis. *EMBO J* 1994; 13: 1255–62.
25. Perrakis A, Harkiolaki M, Wilson KS, *et al*. ARP/wARP and molecular replacement. *Acta Crystallogr D Biol Crystallogr* 2001; 57: 1445–50.
26. Emsley P, Cowtan K. Coot: model-building tools for molecular graphics. *Acta Crystallogr D Biol Crystallogr* 2004; 60: 2126–32.
27. Murshudov GN, Vagin AA, Dodson EJ. Refinement of macromolecular structures by the maximum-likelihood method. *Acta Crystallogr D Biol Crystallogr* 1997; 53: 240–55.
28. Kumar P, Henikoff S, Ng PC. Predicting the effects of coding non-synonymous variants on protein function using the SIFT algorithm. *Nat Protoc* 2009; 4: 1073–81.
29. Hurst JM, McMillan LEM, Porter CT, *et al*. The SAAPdb web resource: a large-scale structural analysis of mutant proteins. *Hum Mutat* 2009; 30: 616–24.
30. Consortium U. Reorganizing the protein space at the universal Protein resource (UniProt). *Nucleic Acids Res* 2012; 40: D71–5.
31. Ng PC, Henikoff S. Accounting for human polymorphisms predicted to affect protein function. *Genome Res* 2002; 12: 436–46.
32. Cargill M, Altshuler D, Ireland J, *et al*. Characterization of single-nucleotide polymorphisms in coding regions of human genes. *Nat Genet* 1999; 22: 231–8.
33. Wiel L, Venselaar H, Veltman JA, *et al*. Aggregation of population-based genetic variation over protein domain homologues and its potential use in genetic diagnostics. *Hum Mutat* 2017; 38: 1454–63.
34. Vihinen M. Types and effects of protein variations. *Hum Genet* 2015; 134: 405–21.
35. David A, Sternberg MJE. The contribution of missense mutations in core and rim residues of protein–protein interfaces to human disease. *J Mol Biol* 2015; 427: 2886–98.
36. Bürgisser DM, Thöny B, Redweik U, *et al*. 6-pyruvoyl tetrahydropterin synthase, an enzyme with a novel type of active site involving both zinc binding and an intersubunit catalytic triad motif; Site-directed mutagenesis of the proposed active center, characterization of the metal binding site and modelling of substrate binding. *J Mol Biol* 1995; 253: 358–69.
37. Brasil S, Viecelli HM, Meili D, *et al*. Pseudoexon exclusion by antisense therapy in 6-pyruvoyl-tetrahydropterin synthase deficiency. *Hum Mutat* 2011; 32: 1019–27.
38. Meili D, Kralovicova J, Zagalak J, *et al*. Disease-causing mutations improving the branch site and polypyrimidine tract: pseudoexon activation of LINE-2 and antisense Alu lacking the poly(T)-tail. *Hum Mutat* 2009; 30: 823–31.
39. Leuzzi V, Carducci C, Carducci C, *et al*. Phenotypic variability, neurological outcome and genetics background of 6-pyruvoyl-tetrahydropterin synthase deficiency. *Clin Genet* 2010; 77: 249–57.
40. Vatanavicharn N, Kuptanon C, Liammongkolkul S, *et al*. Novel mutation affecting the pterin-binding site of PTS gene and review of PTS mutations in Thai patients with 6-pyruvoyltetrahydropterin synthase deficiency. *J Inherit Metab Dis* 2009; 32 (Suppl 1): S279–82.
41. Żekanowski C, Nowacka M, Sendecka E, *et al*. Identification of mutations causing 6-pyruvoyl-tetrahydrobiopterin synthase deficiency in Polish patients with variant hyperphenylalaninemia. *Mol Diagn* 1998; 3: 237–9.
42. Dong C, Wei P, Jian X, *et al*. Comparison and integration of deleteriousness prediction methods for nonsynonymous SNVs in whole exome sequencing studies. *Hum Mol Genet* 2015; 24: 2125–37.
43. Bendl J, Stourac J, Salanda O, *et al*. PredictSNP: robust and accurate consensus classifier for prediction of disease-related mutations. *PLoS Computat Biol* 2014; 10. e1003440.
44. Hicks S, Plon SE, Kimmel M. Statistical analysis of missense mutation classifiers. *Hum Mutat* 2013; 34: 405–6.
45. Guex N, Peitsch MC. SWISS-MODEL and the Swiss-Pdb Viewer: an environment for comparative protein modeling. *Electrophoresis* 1997; 18: 2714–23.
46. Gao M, Zhou H, Skolnick J. Insights into disease-associated mutations in the human proteome through protein structural analysis. *Structure* 2015; 23: 1362–9.
47. Mueller SC, Backes C, Kalinina OV, *et al*. BALL-SNP: combining genetic and structural information to identify candidate non-synonymous single nucleotide polymorphisms. *Genome Med* 2015; 7: 65.